AL-Fatlawy | Article 11840
J Pure Appl Microbiol. 2026. doi: 10.22207/JPAM.20.3.33
Received: 20 May 2026 | Accepted: 03 August 2026

P-ISSN: 0973-7510; E-ISSN: 2581-690X

RESEARCH ARTICLE OPEN ACCESS

Molecular Docking Analysis of Coumarin and Indole Derivatives Targeting the MexB and GyrB in Multidrug-resistant *Pseudomonas aeruginosa* Clinical Isolates

Hawraa Natiq Kabroot AL-Fatlawy

Medical Microbiology, College of Medicine, University of Kufa, Najaf, Iraq.

Abstract

Multidrug-resistant (MDR) *Pseudomonas aeruginosa* has emerged as a significant clinical threat due to its high resistance to multiple antibiotic classes and the limited effectiveness of current therapeutic options. This study aimed to evaluate selected coumarin and indole derivatives targeting the MexB and GyrB proteins of MDR *P. aeruginosa* using an integrated in silico approach, supported by molecular characterization of clinical isolates. A total of 44 clinical *P. aeruginosa* isolates recovered from sputum, urine, wound swabs, and burn swabs were examined for antimicrobial susceptibility, revealing extensive drug resistance. Complete resistance (100%) was observed against amoxicillin-clavulanic acid (AMC), cefotaxime (CTX), and trimethoprim-sulfamethoxazole (SXT). Resistance rates were 97.7% for ticarcillin-clavulanic acid (TIM), 88.63% for amikacin (AK), 60% for imipenem (IMP) and meropenem (MEM), and 52.27% for ciprofloxacin (CIP) and levofloxacin (LEV). PCR analysis confirmed the presence of the *GyrB* and *MexB* genes in all isolates. Representative PCR-positive isolates were sequenced and verified by BLAST analysis. The nucleotide sequence of the *GyrB* gene has been deposited in the DDBJ under accession number LC919849, and the corresponding protein sequence was assigned GenBank accession number BHR60112.1. Molecular modeling and structural validation of the GyrB and MexB proteins were performed prior to molecular docking analysis. Novobiocin and PAβN were selected as reference inhibitors for GyrB and MexB, respectively, while coumarin- and indole-based compounds were evaluated as candidate ligands. Docking analysis revealed strong predicted binding affinities for novobiocin (-10.2 kcal/mol) and PAβN (-8.1 kcal/mol). The coumarin derivative exhibited favorable predicted interactions within the ATP-binding pocket of GyrB, whereas the indole derivative demonstrated favorable predicted binding within the substrate-binding cavity of MexB. ADMET and toxicity analyses indicated favorable predicted drug-likeness for both compounds, with high gastrointestinal absorption, no bioavailability violations, and a score of 0.55. However, the indole derivative showed a positive AMES test prediction, indicating potential mutagenic liability. Molecular dynamics simulations demonstrated the structural stability of the modeled MexB protein over a 25 ns simulation period. Overall, these findings provide preliminary in silico evidence supporting further investigation of coumarin and indole derivatives as candidate compounds targeting GyrB and MexB in MDR *P. aeruginosa*.

Keywords: MDR *Pseudomonas aeruginosa*, Targeting GyrB and MexB, Efflux Pump Inhibition, In Silico Drug Discovery, Antibacterial Agents, Coumarin Derivatives, Indole Derivatives, Molecular Modeling

Correspondence: hawraan.alfatlawy@uokufa.edu.iq

Citation: AL-Fatlawy HNK. Molecular Docking Analysis of Coumarin and Indole Derivatives Targeting the MexB and GyrB in Multidrug-resistant *Pseudomonas aeruginosa* Clinical Isolates. *J Pure Appl Microbiol.* Published online 29 August 2026. doi: 10.22207/JPAM.20.3.33

INTRODUCTION

Pseudomonas aeruginosa is considered one of the most clinically significant opportunistic pathogens associated with hospital-acquired infections, particularly in immunocompromised patients. The rapid emergence of multidrug-resistant (MDR) strains has become a major global health concern due to the reduced effectiveness of conventional antibiotics and the increasing prevalence of resistance mechanisms.[1,2]

Among the major mechanisms contributing to antimicrobial resistance in *P. aeruginosa* are target modification, enzymatic drug inactivation, reduced membrane permeability, and the overexpression of multidrug efflux pumps. Notably, the Resistance-Nodulation-Division (RND) family efflux system MexAB-OprM plays a critical role in antibiotic extrusion and MDR phenotype development, where MexB functions as the principal inner membrane transporter responsible for substrate recognition and binding.[3,4] In parallel, DNA gyrase subunit B (GyrB) remains an important antibacterial target due to its essential role in DNA replication and bacterial survival. Inhibition of GyrB disrupts ATP-dependent DNA supercoiling, making it an attractive target for antibacterial drug discovery.[5,6]

The continuous rise in antibiotic resistance has accelerated the application of computer-aided drug design (CADD) approaches to identify novel antibacterial compounds. Molecular docking has become one of the most widely used in silico techniques for evaluating protein-ligand interactions, predicting binding affinities, and identifying potential inhibitors prior to experimental validation.[3,7] Furthermore, molecular dynamics (MD) simulations provide additional insights into the structural stability and dynamic behavior of protein-ligand complexes under simulated physiological conditions through analyses such as root mean square deviation (RMSD), root mean square fluctuation (RMSF), radius of gyration (Rg), hydrogen bonding, and solvent-accessible surface area (SASA).[8]

In recent years, natural product-derived scaffolds, such as coumarin and indole derivatives, have attracted considerable attention as promising antibacterial agents due to their broad biological activities and favorable pharmacological properties. Coumarin-based compounds have been reported to exhibit antibacterial and enzyme inhibitory activities, particularly against bacterial gyrase targets, while indole derivatives have demonstrated potential as efflux pump inhibitors and antimicrobial agents.[9,10]

In silico pharmacokinetic and toxicity prediction methods including absorption, distribution, metabolism, excretion, and toxicity (ADMET) analysis are increasingly integrated into early-stage drug discovery to improve candidate selection and reduce the probability of clinical failure. Drug-likeness evaluation based on Lipinski's Rule of Five, gastrointestinal (GI) absorption, bioavailability, and toxicity predictions provides valuable information regarding the pharmacological suitability of candidate compounds before experimental studies.[11]

Therefore, the present study aims to evaluate the interactions of selected coumarin and indole derivatives with the GyrB and MexB proteins of *P. aeruginosa* clinical isolates using an integrated molecular modeling and in silico approach. The study include protein modeling and validation, molecular docking of reference and candidate ligands, protein-ligand interaction analysis, and ADMET and toxicity prediction, as well as MD simulation of the modeled MexB protein.

MATERIALS AND METHODS

Clinical isolates and bacterial identification

A total of 613 clinical specimens including sputum, urine, wound swabs, and burn swabs were collected from hospitalized patients with suspected bacterial infections in Najaf and Karbala hospitals, Iraq, between March 2024 and April 2025. All molecular diagnostic analyses were performed at the Molecular Postgraduate Laboratory, Faculty of Medicine, University of Kufa, Iraq. Only non-duplicate clinical isolates were included in the study; duplicate isolates recovered from the same patient and contaminated cultures were excluded. A total of 44 clinical isolates of *P. aeruginosa* were recovered from different clinical specimens and selected for further investigation. Primary isolation and identification were performed using standard microbiological procedures, including colony morphology assessment, Gram staining,

and conventional biochemical tests. Species-level identification was subsequently confirmed using the VITEK 2 Compact automated identification system (bioMerieux, France) according to the manufacturer's instructions.

Antimicrobial susceptibility testing

Antimicrobial susceptibility testing was performed using the Kirby-Bauer disk diffusion method on Mueller-Hinton agar, following standard procedures. The inhibition zone diameters were interpreted according to the Clinical and Laboratory Standards Institute (CLSI) guidelines (CLSI M100, 35th edition, 2025).[12] The antimicrobial agents tested included amoxicillin-clavulanic acid (AMC, 30 µg), ticarcillin-clavulanic acid (TIM, 75 µg), cefotaxime (CTX, 30 µg), imipenem (IMP, 10 µg), meropenem (MEM, 10 µg), amikacin (AK, 30 µg), ciprofloxacin (CIP, 5 µg), levofloxacin (LEV, 5 µg), and trimethoprim-sulfamethoxazole (SXT, 25 µg). *Escherichia coli* ATCC 25922 was used as the quality control strain. Isolates were classified as MDR if they exhibited non-susceptibility to at least one agent in three or more antimicrobial classes.

Molecular detection of target genes

Genomic DNA was extracted using a commercial bacterial DNA extraction kit (Promega, USA) according to the manufacturer's instructions. Polymerase chain reaction (PCR) amplification was performed to detect the *GyrB* and *MexB* genes using gene-specific primers. For the *GyrB* gene, the forward primer sequence was 5'-AGGAAGAAGGGGTTTCTGCG-3' and the reverse primer sequence was 5'-TCCGGTACCTTCACCGAGAT-3', generating an expected amplicon of 736 bp. PCR amplification was performed using the following cycling conditions: initial denaturation at 94 °C for 3 min; 30 cycles of 94 °C for 45 sec, 59 °C for 45 sec, and 72 °C for 45 sec; followed by a final extension at 72 °C for 5 min. For the *MexB* gene, the forward primer sequence was 5'-GAAGAACTTCCTCATGGTGGTC-3', and the reverse primer sequence was 5'-GAGGGTCTTCACTACCTCATGG-3', producing an expected amplicon of 727 bp MexB. The cycling conditions were as follows: initial denaturation at 94 °C for 3 min; 30 cycles of 94 °C for 45 sec, 58 °C for 45 sec, and 72 °C for 45 sec; followed by a final extension at 72 °C for 5 min.[13]

Sequence analysis and phylogenetic tree construction

Representative PCR-positive isolates were selected for sequencing to confirm the identity of the amplified target genes. A total of 10 isolates were sequenced, including six GyrB and four MexB isolates. The obtained nucleotide sequences were analyzed using the BLAST program available through the National Center for Biotechnology Information (NCBI) database to determine sequence identity with reference sequences. The representative GyrB sequence was deposited in the DNA Data Bank of Japan (DDBJ) database under accession number LC919849. Sequence alignments were performed using NCBI databases.

Phylogenetic analysis was constructed based on the nucleotide sequences of the *GyrB* gene using the NCBI Phylogenetic Tree tool with the Fast Minimum Evolution method to determine the genetic relationships between clinical *P. aeruginosa* isolates and reference strains retrieved from the NCBI database.

Protein modeling and validation

Protein sequences were generated using the NCBI open reading frame (ORF) Finder tool. Three-dimensional structural models of the GyrB and MexB proteins were generated using the SWISS-MODEL server, based on the best available AlphaFold reference models. The GyrB model was generated using the AlphaFold model Q917C2.1.A, whereas the MexB model was derived from the AlphaFold model A0A5K1SFB4.1.A. Model quality was assessed using the GMQE score provided by SWISS-MODEL. Structural quality and stereochemical validation were further evaluated through MolProbity analysis, Ramachandran plot assessment, clash score, and side-chain geometry analysis. Additionally, the predicted oligomeric state and structural features, including transmembrane regions where applicable, were considered before molecular docking analysis.[14]

Ligand selection and preparation

Reference and candidate ligands were selected based on their previously reported antibacterial activity and inhibitory effects against the corresponding target proteins. Novobiocin and phenylalanine-arginine β-naphthylamide (PAβN) were selected as reference inhibitors for

GyrB and MexB, respectively, while a coumarin derivative and an indole derivative were selected as candidate ligands. The chemical structures, PubChem Compound Identification (CID) numbers, molecular descriptors, and SMILES notations were retrieved from the PubChem database. Ligand structures were prepared using Discovery Studio Visualizer (DSV) and subjected to geometry optimization before molecular docking analysis.[15]

Molecular docking analysis

Molecular docking analysis was performed using the CB-Dock2 platform, which integrates AutoDock Vina to evaluate ligand binding affinity to target proteins. Protein preparation included the removal of water molecules, addition of hydrogen atoms, and structural optimization prior to docking. Ligands were prepared using DSV and subjected to geometry optimization before docking. The CB-Dock2 platform automatically identified multiple potential binding cavities and generated corresponding docking parameters, including cavity center coordinates and docking box dimensions. Docking was performed within the predicted cavities, and the cavity with the lowest binding energy was selected for subsequent interaction analysis. Protein-ligand interactions were visualized using DSV.[16,17]

ADMET and toxicity prediction

Pharmacokinetic properties and drug-likeness of the candidate ligands were predicted using the SwissADME web server. Physicochemical properties assessed included molecular weight (MW), topological polar surface area (TPSA), consensus LogP, GI absorption, Lipinski's rule of five, bioavailability score, PAINS alerts, and Brenk structural alerts. Toxicity predictions were performed using the pkCSM online platform and encompassed AMES mutagenicity, maximum tolerated dose (MTD), oral rat acute toxicity (LD50), oral rat chronic toxicity (LOAEL), hepatotoxicity, hERG I/II inhibition, and skin sensitization. The in silico ADMET and toxicity predictions obtained served as preliminary screening tools to prioritize candidate compounds for further investigation and were not considered definitive evidence of their pharmacological safety or toxicity.[18,19]

Molecular dynamics simulation of the MexB protein

MD simulations were performed on the MexB protein using the WebGRO platform to evaluate its structural stability under physiological conditions. The simulations employed the GROMOS96 54a7 force field with the SPC water model within a triclinic simulation box. The system was neutralized by adding 0.15 M NaCl. Energy minimization was performed using the Steepest Descent algorithm for 5,000 steps. System equilibration was conducted under NVT and NPT ensembles at a temperature of 300 K and a pressure of 1.0 bar, followed by a 25 ns production run using the leapfrog integrator. Structural stability and dynamic behavior were evaluated by analyzing the RMSD, RMSF, Rg, SASA, and hydrogen bond profiles throughout the simulation period.[20]

Statistical analysis

Statistical analysis was performed using SPSS software Version 26 and Microsoft Excel 2021.[21] Descriptive statistics were expressed as frequencies and percentages to summarize the distribution of MDR *P. aeruginosa* isolates and the prevalence of the resistance determinants investigated.[22]

Ethical approval

This study was conducted in accordance with the ethical principles outlined in the Declaration of Helsinki. Ethical approval was obtained from the Medical Ethics Committee, Faculty of Medicine, University of Kufa, Iraq (Approval No. MEC-169, approved on 19 May 2025). All procedures involving clinical specimens were performed in compliance with institutional ethical guidelines, and patient confidentiality was strictly maintained throughout the study.

RESULTS

Clinical characteristics, sample distribution, and identification of *Pseudomonas aeruginosa*

A total of 613 clinical specimens were collected from patients with suspected bacterial infections, including sputum, urine, wound swabs, and burn samples, representing a broad range of

infection sites. Following primary culturing and initial phenotypic screening, 44 isolates (7.2%) were identified as *P. aeruginosa* (Table 1). The presumptive identification of *P. aeruginosa* was based on characteristic colony morphology, pigmentation patterns, and Gram-staining features consistent with Gram-negative, non-fermentative bacilli. Species-level confirmation was subsequently achieved using the VITEK2 ND automated identification system, which showed complete concordance with the phenotypic findings. These clinically confirmed isolates were selected for subsequent antimicrobial susceptibility testing, molecular characterization of gyrase-associated genes, and downstream in silico analyses.

Antimicrobial susceptibility profiles of clinical *Pseudomonas aeruginosa* isolates

Antimicrobial susceptibility testing of the 44 clinical *P. aeruginosa* isolates revealed a high level of resistance across multiple antibiotic classes. Notably, elevated resistance was observed against β-lactam/β-lactamase inhibitor combinations, cephalosporins, carbapenems, aminoglycosides, fluoroquinolones, and folate pathway inhibitors. A detailed summary of resistance rates for each tested antimicrobial agent is presented in Table 2.

Overall, the resistance profiles demonstrated non-susceptibility to agents from six distinct antimicrobial categories, fulfilling the established criteria for MDR. Furthermore, the broad resistance distribution indicates that a substantial proportion of the isolates exhibited patterns consistent with an extensively drug-resistant phenotype.

Molecular detection and sequence confirmation of target genes

Molecular screening using PCR revealed the presence of *MexB* and *GyrB* genes in all 44 clinical *P. aeruginosa* isolates, confirming their universal distribution among the examined strains. The consistent detection of these target genes

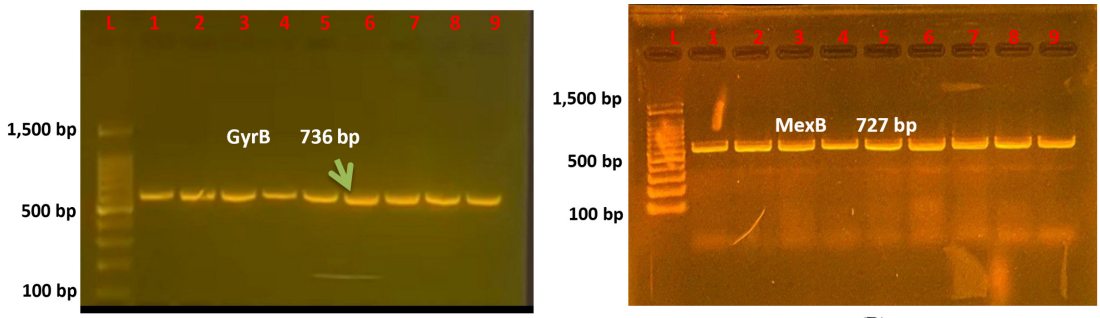

Figure 1. Representative PCR Amplification of Target Genes in Clinical *Pseudomonas aeruginosa* Isolates
(A) Amplification of the *GyrB* gene showing the expected band size (736 bp)
(B) Amplification of the *MexB* gene (727 bp) demonstrating clear and specific product amplification.
L: DNA ladder (100 bp); lanes 1-9: representative positive clinical isolates.

Table 1. Distribution of Clinical Specimens and Isolation Rates of *P. aeruginosa*

Specimen Type	Total Samples (n = 613)	Total Samples (%)	*P. aeruginosa* Isolates (n = 44)	Isolation Rate within Specimen Type (%)
Urine	342	55.8	23	6.7
Sputum	130	21.2	12	9.2
Burn samples	76	12.4	4	5.3
Wound samples	65	10.6	5	7.7
Total	613	100	44	7.2 (overall)

across all isolates underscores their essential role in bacterial viability and validates their selection for further molecular and in silico analyses. Representative PCR amplification profiles of the *GyrB* and *MexB* genes are shown in Figure 1.

For sequence-level characterization, a representative subset of 10 PCR-positive isolates was selected for sequence analysis, including six isolates for the *GyrB* gene and four isolates for *MexB*. DNA sequencing was performed by Macrogen (South Korea). The obtained sequences were analyzed using the BLAST algorithm available through NCBI to confirm gene identity and sequence similarity before performing multiple sequence alignment, mutation assessment, and protein structure modeling. The nucleotide sequence of the *GyrB* gene was deposited in the DDBJ under accession number LC919849, and the corresponding protein sequence was assigned GenBank accession number BHR60112.1.

Genetic variability, sequence analysis, and phylogenetic analysis of the *GyrB* gene

Sequence analysis of the *GyrB* gene revealed a high degree of similarity to *P. aeruginosa* reference sequences available in the NCBI database. BLAST analysis demonstrated sequence identities ranging from 95%-99%, indicating that the *GyrB* gene is highly conserved among the examined clinical isolates.

Multiple sequence alignment further confirmed the conserved nature of the analyzed coding region, with no significant insertions or deletions detected. Although minor nucleotide variations were observed, these changes did not affect the conserved functional motifs of DNA GyrB. The translated protein sequence (GenBank accession No. BHR60112.1), derived from the deposited GyrB nucleotide sequence (DDBJ accession No. LC919849), retained the conserved ATP-binding and catalytic domains characteristic

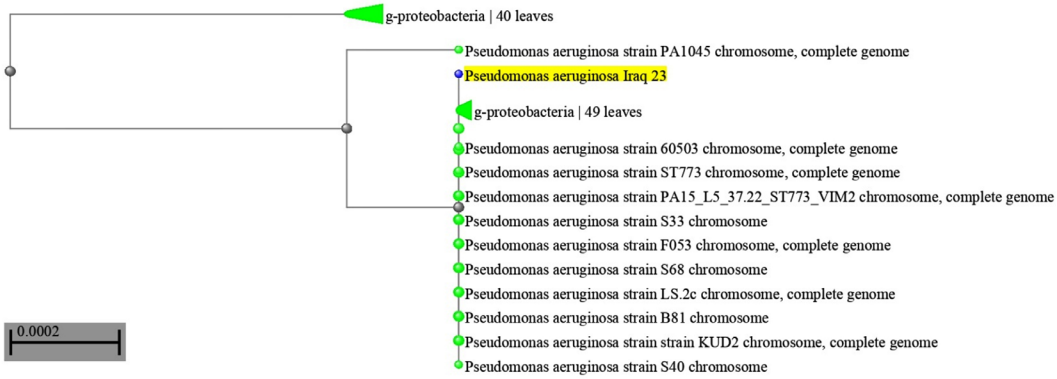

Figure 2. NCBI Phylogenetic Tree of the *GyrB* Gene in *Pseudomonas aeruginosa*

Table 2. Resistance Rates of Clinical *P. aeruginosa* Isolates (n = 44)

Antibiotic	Antimicrobial Class	Resistant Isolates (%)
Amoxicillin-clavulanic acid (AMC)	β-lactam	44 (100%)
Ticarcillin-clavulanic acid (TIM)	β-lactam	43 (97.72%)
Cefotaxime (CTX)	Cephalosporin	44 (100%)
Imipenem (IMP)	Carbapenem	26 (60%)
Meropenem (MEM)	Carbapenem	26 (60%)
Amikacin (AK)	Aminoglycoside	39 (88.63%)
Ciprofloxacin (CIP)	Fluoroquinolone	23 (52.27%)
Levofloxacin (LEV)	Fluoroquinolone	23 (52.27%)
Trimethoprim-sulfamethoxazole (SXT)	Folate Inhibitor	44 (100%)

of *GyrB*, supporting its suitability as a stable molecular target for inhibitor binding.

Phylogenetic analysis of the *GyrB* gene demonstrated that the representative clinical isolates clustered closely with reference *P. aeruginosa* strains retrieved from the NCBI database, indicating a high level of genetic conservation and confirming the molecular identity of the studied isolates (Figure 2). These findings further support the use of the *GyrB* gene as a reliable molecular marker and a suitable target for subsequent computational analyses.

The phylogenetic tree based on *GyrB* gene nucleotide sequences shows the clustering of representative clinical isolates (highlighted) alongside reference *P. aeruginosa* strains retrieved from the NCBI database. The phylogenetic tree was constructed using the Fast Minimum Evolution method. The scale bar (0.0002) represents the evolutionary distance, expressed as the number of nucleotide substitutions per site.

Protein preparation, structural modeling, and validation of target proteins

The three-dimensional structures of the target proteins, GyrB and MexB, were prepared for molecular docking analysis. The GyrB nucleotide sequence obtained from *P. aeruginosa* isolates

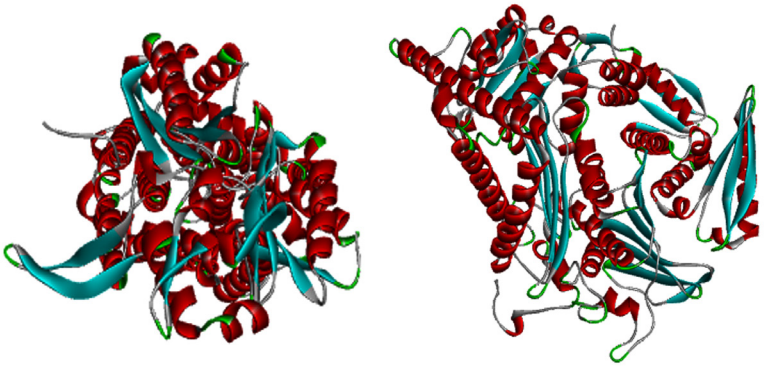

Figure 3. Three-Dimensional Structural Models of the GyrB and MexB Proteins
Three-dimensional structural models of GyrB and MexB were generated using the SWISS-MODEL server and validated through MolProbity analysis.
(A) The GyrB protein model shows excellent stereochemical quality.
(B) The MexB protein model demonstrates good structural reliability and accurately predicts the transmembrane region.
The validated models were optimized and subsequently used for molecular docking analysis and MD simulation.

Table 3. Chemical Characteristics of Reference Inhibitors and Candidate Ligands

Ligand	PubChem CID	Molecular Formula	Molecular Weight (g/mol)	SMILES
Novobiocin	54675769	$C_{31}H_{36}N_2O_{11}$	612.60	CC1=C(C=CC2=C1OC(=O)C(=C2O)NC(=O)C3=CC(=C(C=C3)O)CC=C(C)C)O[C@H]4[C@@H]([C@@H]([C@H](C(O4)(C)C)OC)OC(=O)N)O
Coumarin derivative	13295	$C_{15}H_{11}NO_3$	253.25	COC1=CC2=C(C=C1)C(=CC(=O)O2)C3=CC=NC=C3
PAβN	90665180	$C_{25}H_{32}Cl_2N_6O_2$	519.50	C1=CC=C(C=C1)C[C@@H](C(=O)N[C@@H](CCCN=C(N)N)C(=O)NC2=CC3=CC=CC=C3C=C2)N.Cl.Cl
Indole derivative	589138	$C_{15}H_{12}N_2O$	236.27	C1=CC=C(C=C1)NC(=O)C2=CC3=CC=CC=C3N2

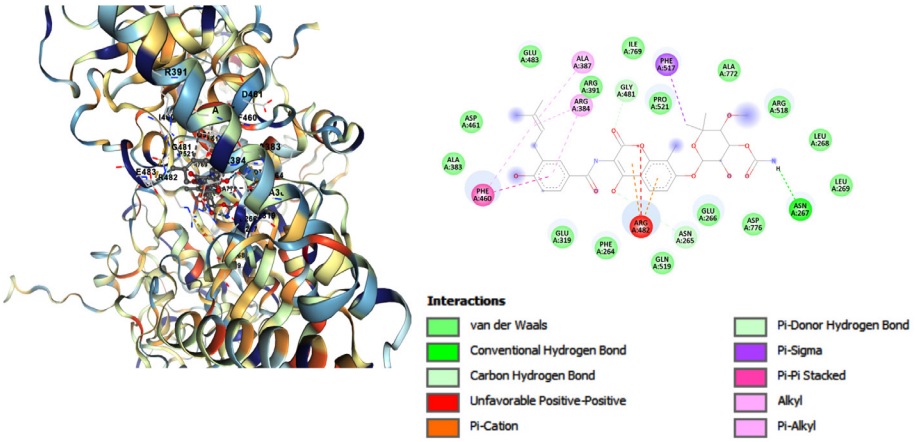

(A) GyrB-novobiocin complex and key interactions

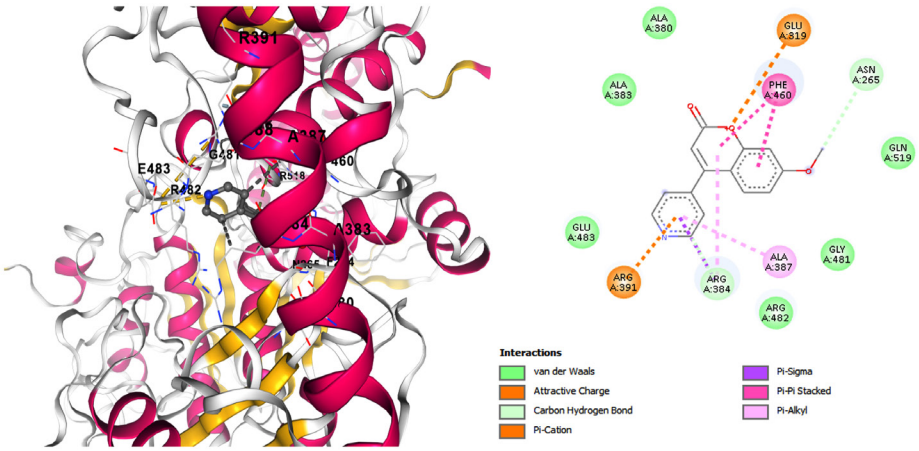

(B) GyrB-coumarin complex and key interactions

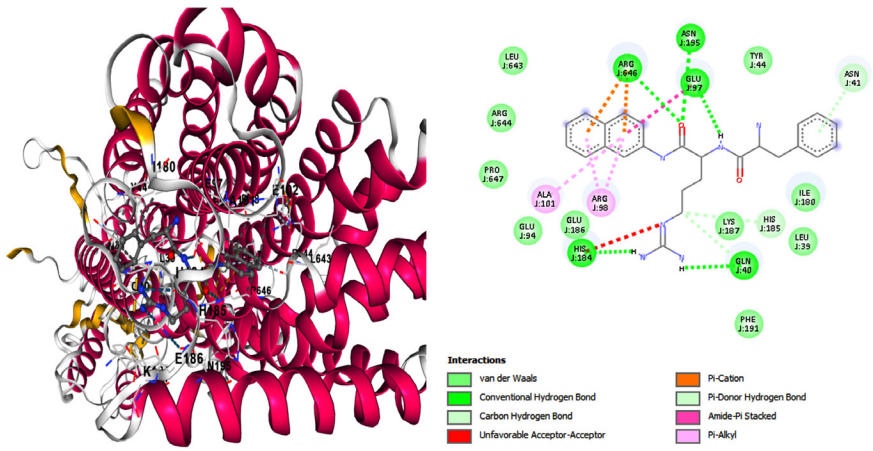

(C) MexB-PAβN complex and key interactions

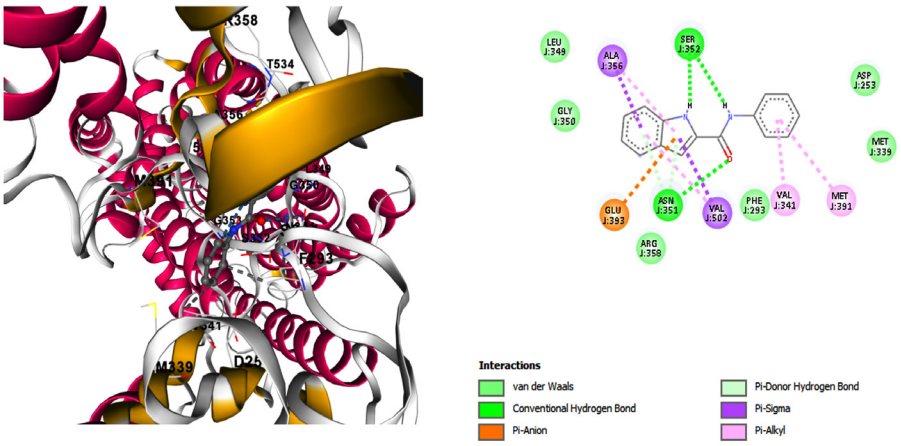

(D) MexB-indole complex and key interactions

Figure 4. Protein-Ligand Interaction Analysis of GyrB and MexB Complexes
Two-dimensional (2D) and three-dimensional (3D) representations of protein-ligand interactions are shown. (A) GyrB-Novobiocin complex, (B) GyrB-Coumarin complex, (C) MexB-PAβN complex, and (D) MexB-Indole complex. Key interactions, including hydrogen bonds, π-interactions, and hydrophobic contacts, are illustrated within the binding sites

Table 4. Reference Inhibitors and Candidate Ligands Selected for Molecular Docking and ADMET Analysis

Target Protein	Reference Inhibitor	Candidate Ligand	Chemical/Functional Class
GyrB	Novobiocin	Coumarin derivative	ATP-binding/Gyrase inhibitor
MexB	PAβN	Indole derivative	Efflux pump inhibitors

was translated into its corresponding amino acid sequence based on the predicted ORF. The translated protein sequence (GenBank accession No. BHR60112.1), derived from the deposited GyrB nucleotide sequence (DDBJ accession No. LC919849), was subsequently used for structural modeling. Three-dimensional structural models of GyrB and MexB were generated using the SWISS-MODEL server, based on the best available AlphaFold reference models. The GyrB model was generated using the AlphaFold reference model Q917C2.1.A, which has 100% sequence identity, a GMQE score of 0.88, and a predicted monomeric oligomeric state. Structural validation using MolProbity demonstrated excellent model quality, with a MolProbity score of 0.58, a clash score of 0.00, and 97.64% of residues located in favored regions of the Ramachandran plot.

The MexB model was generated using the AlphaFold reference model A0A5K1SFB4.1.A, which has 100% sequence identity, a GMQE score of 0.91, and a QMEAN score of 0.89 ± 0.05, and is predicted to be monomeric. The model exhibits 60% sequence similarity across the entire protein length (residues 1-721), indicating a robust and complete structural model suitable for docking analysis. Additionally, the model is predicted to contain a transmembrane segment, consistent with the membrane-associated nature of MexB.

Protein preparation involved adding hydrogen atoms and performing structural optimization through energy minimization to ensure model stability. Active binding sites were identified based on conserved functional domains, particularly the ATP-binding pocket of GyrB and the substrate-binding catalytic site of MexB. The modeled three-dimensional structures of GyrB and MexB are presented in Figure 3A and B.

Selection, structural classification, and ADMET profiling of candidate ligands

A panel of reference inhibitors and candidate ligands was selected for molecular docking analysis against GyrB and MexB. The selection strategy included established reference inhibitors as well as structurally related candidate ligands selected based on previously reported antibacterial activity and their potential to interact with conserved functional regions of the

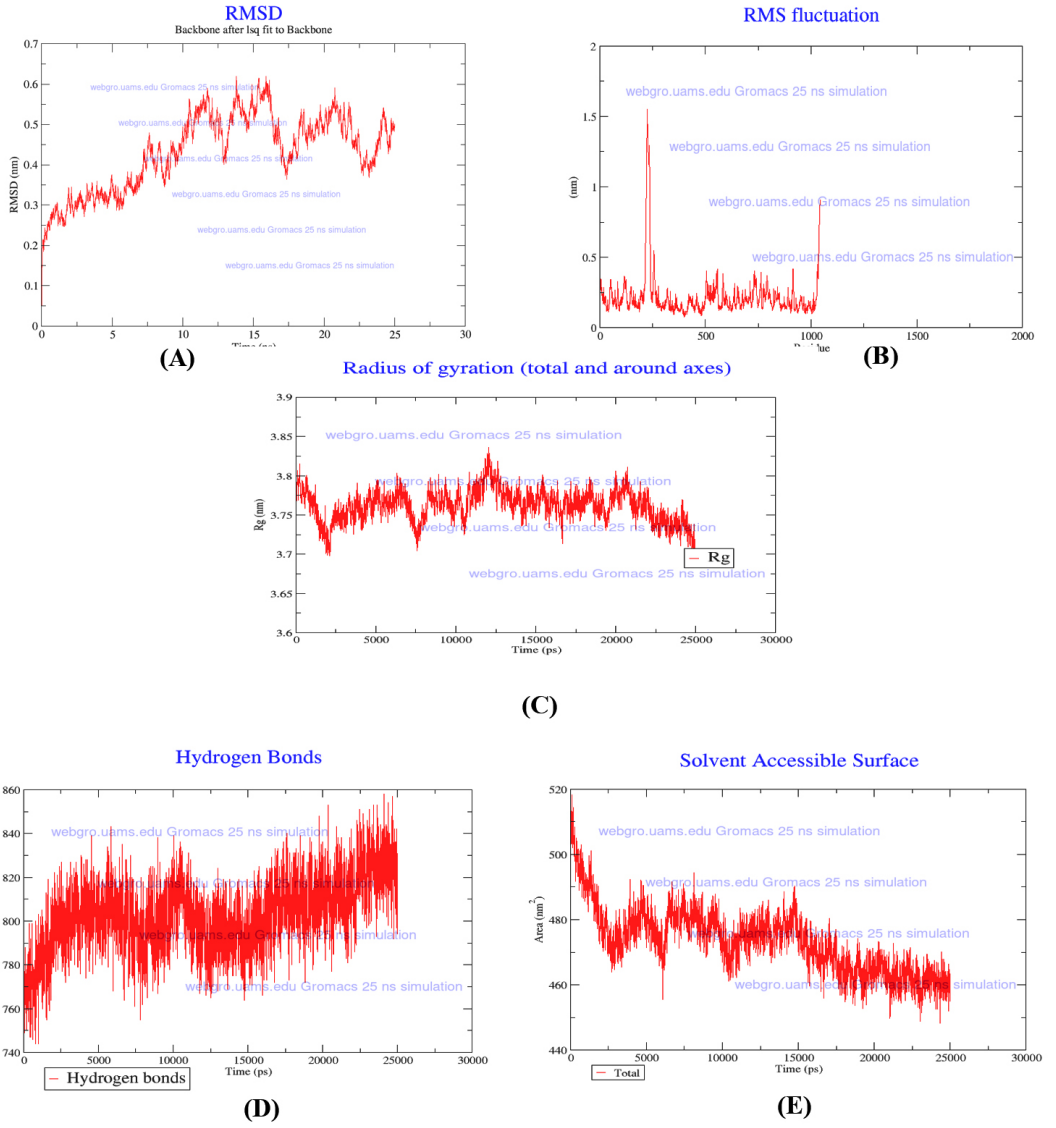

Figure 5. Molecular Dynamics Simulation Analysis of the MexB Protein
(A) RMSD of the MexB protein
(B) RMSF of the MexB protein
(C) Rg of the MexB protein
(D) Intramolecular hydrogen bonds of the MexB protein
(E) SASA of the MexB protein
The plots illustrate the structural stability, residue flexibility, compactness, intramolecular hydrogen-bonding network, and solvent accessibility of the MexB protein throughout the 25 ns MD simulation

respective target proteins. The selected ligands were classified according to their target specificity and chemical class. The chemical structures, PubChem CID numbers, molecular formulas, MWs, and SMILES notations of the selected ligands are summarized in Table 3. Novobiocin and PAbN were used as reference inhibitors for *GyrB* and *MexB*, respectively, while a coumarin derivative and an indole derivative were evaluated as candidate ligands (Table 4).

Prior to docking, ligand structures were retrieved from the PubChem database, prepared using DSV, and subjected to geometry optimization. Drug-likeness and pharmacokinetic properties were subsequently evaluated through in silico ADMET analysis, which included assessments of physicochemical characteristics, Lipinski's rule of five parameters, GI absorption, bioavailability, and toxicity prediction. This integrated approach enabled the prioritization of candidate ligands based on both their predicted binding affinity and favorable pharmacokinetic profiles.

Molecular docking validation using reference inhibitors

To validate the molecular docking protocol, established reference inhibitors were used for each target protein. Novobiocin and PAβN were selected as reference ligands for GyrB and MexB, respectively. Both reference inhibitors exhibited favorable binding affinities and stable interactions within the functional binding sites of their respective proteins. Novobiocin bound to the ATP-binding pocket of *GyrB*, whereas PAβN

Table 5. Molecular Docking Results and Predicted Binding Cavity Parameters for Selected Ligands Targeting GyrB and MexB

Target Protein	Ligand	Type	Best Pocket	Binding Energy (kcal/mol)	Cavity Volume (Å3)	Center (x, y, z)	Docking Size (x, y, z)
GyrB	Novobiocin	Control	C1	-10.2	7174	(-16, -2, 8)	(35, 29, 35)
GyrB	Methoxy-4 (4-pyridyl) Coumarin	Candidate	C1	-8.2	7174	(-16, -2, 8)	(35, 34, 35)
MexB	PAβN	Control	C4	-8.1	428	(276, 316, 186)	(24, 24, 24)
MexB	N-phenyl-1H-indole-2-Carboxamide	Candidate	C1	-7.7	6691	(291, 310, 241)	(33, 27, 35)

Table 6. Key Interaction Residues in Protein-Ligand Complexes

Target	Ligand	Type	Key Hydrogen Bonds	π-Interactions	Hydrophobic Contacts	Notable Residues
GyrB	Novobiocin	Control	Asn267	Arg482 (π-cation), Phe460 (π-π)	Ala387 Arg384 Arg391	Glu483 Gly481 Pro521
GyrB	Coumarin	Candidate	Asn265	Arg391 (π-cation), Phe460 (π-π)	Ala387 Arg384	Glu483 Arg482 Ile769
MexB	PAβN	Control	Glu97 His184 Glu40	Arg46 (π-cation), Glu97 (amide-π)	Ala101 Arg98	Tyr44 Ile180 Phe191
MexB	Indole	Candidate	Ser352 Asn351 Arg358	Glu393 (π-anion)	Ala356 Val502 Met391	Leu349 Gly350 Asp253

Table 7. Predicted In Silico ADMET and Toxicity Properties of Selected Candidate Coumarin and Indole Derivative Ligands

Ligand	MW (g/mol)	TPSA (Å2)	Consensus LogP	GI Absorption	Lipinski	Bio-availability	PAINS	Brenk	AMES	MTD Human	LD_{50} Rat	LOAEL Rat	Hepato-toxicity	hERG I/II	Skin Sensitization
Coumarin derivative	253.25	52.33	2.55	High	Yes (0 violations)	0.55	0	1	Yes	-0.61	2.345	1.617	No	No/No	No
Indole derivative	236.27	44.89	2.90	High	Yes (0 violations)	0.55	0	0	No	-0.259	2.563	0.953	No	No/No	No

MTD Human: Maximum tolerated dose in humans (log mg/kg/day); LD50 Rat: Oral acute toxicity in rats (mol/kg); LOAEL Rat: Oral rat chronic toxicity (log mg/kg bw/day)

interacted with the substrate-binding cavity of MexB. These findings confirm the suitability of the docking protocol for the subsequent evaluation of candidate ligands.

Molecular docking results for selected ligands

Molecular docking analysis was performed to evaluate the binding affinity of selected reference inhibitors and candidate ligands against the GyrB and MexB proteins. Multiple binding cavities were automatically predicted for each target protein using the CurPocket platform. The cavity with the lowest predicted binding energy was selected as the optimal binding site for each ligand, and the corresponding cavity parameters are summarized in Table 5.

For GyrB, the reference inhibitor novobiocin exhibited the strongest binding affinity, with a binding energy of -10.2 kcal/mol in the highest-ranked binding pocket (C1). The coumarin derivative also demonstrated favorable binding (-8.2 kcal/mol) within the same pocket, indicating its potential to interact with the ATP-binding site of GyrB. For MexB, the reference inhibitor PAβN showed a binding energy of -8.1 kcal/mol in the top-ranked binding pocket (C4). The indole derivative exhibited a slightly lower binding affinity (-7.7 kcal/mol) but maintained favorable interactions within the predicted binding cavity (C1), suggesting its potential as an efflux pump inhibitor.

Overall, the docking results indicate that GyrB exhibited stronger ligand-binding interactions than MexB. Although the candidate ligands displayed slightly lower binding affinities than their respective reference inhibitors, they showed comparable potential as promising antibacterial lead compounds.

Binding interaction analysis of GyrB and MexB complexes

The protein-ligand interaction analysis was conducted to further evaluate the binding modes and stability of the selected ligands within the active sites of the GyrB and MexB proteins.

For GyrB, the reference inhibitor novobiocin demonstrated a well-established interaction network within the ATP-binding pocket. It formed a conventional hydrogen bond with Asn267, a π-cation interaction with Arg482, and

π-π stacking with Phe460. Additional hydrophobic interactions were observed with residues such as Ala387, along with polar interactions involving Arg384 and Arg391, supported by multiple van der Waals contacts and charged interactions. The coumarin-based candidate ligand exhibited a similar binding orientation within the same pocket, forming a hydrogen bond with Asn265, π-π stacking with Phe460, and a π-cation interaction with Arg391. These interactions indicate that the candidate ligand adopts a binding orientation comparable to that of the reference inhibitor, although it has fewer predicted interactions and a lower predicted binding affinity.

For MexB, the reference inhibitor PAβN formed a robust interaction network within the substrate-binding cavity. It established multiple hydrogen bonds with Glu97, His184, and Gln40, along with a π-cation interaction with Arg46 and amide-π stacking with Glu97. The indole-based candidate ligand exhibited a predicted interaction profile that included hydrogen bonds with Ser352, Asn351, and Arg358, as well as a π-anion interaction with Glu393 and several hydrophobic contacts involving Ala356, Val502, and Met391. However, the predicted interaction network was less extensive than that observed for PAβN.

Overall, the interaction analysis suggested that both candidate ligands could occupy the predicted functional binding sites of their respective targets and establish favorable protein-ligand interactions (Table 6 and Figure 4). Although the candidate ligands displayed slightly lower predicted binding affinities compared to the corresponding reference inhibitors, their binding orientations shared several key interactions with the reference compounds. These docking results provide computational evidence supporting the potential for further investigation; however, they should not be interpreted as direct evidence of inhibitory activity and require experimental validation.

ADMET and toxicity analysis of selected candidate ligands

The pharmacokinetic and drug-likeness properties of the selected candidate ligands were evaluated using in silico ADMET prediction tools. Key parameters analyzed included MW, TPSA, consensus LogP, Lipinski's rule of five compliance, GI absorption, bioavailability score, PAINS alerts, Brenk structural alerts, and predicted toxicity endpoints. The results indicated that both the coumarin and indole derivatives exhibited favorable predicted drug-like characteristics (Table 7). Each compound complied fully with Lipinski's rule of five and was predicted to have high GI absorption. Additionally, both ligands displayed moderate TPSA values (TPSA<60 Å^2), consensus LogP values of 2.55 and 2.90, respectively, and a predicted bioavailability score of 0.55, suggesting favorable physicochemical properties for oral drug candidates.

Neither compound exhibited PAINS alerts; however, the coumarin derivative showed one Brenk structural alert, while the indole derivative showed none. Toxicity predictions indicated that the indole derivative was negative for AMES mutagenicity, hepatotoxicity, hERG I/II inhibition, and skin sensitization. In contrast, the coumarin derivative showed a positive AMES prediction despite its otherwise favorable physicochemical and pharmacokinetic properties, indicating a potential mutagenic liability that warrants careful consideration and further experimental validation.

Overall, the in silico ADMET analysis provides a preliminary computational assessment of the pharmacokinetic and toxicity profiles of the selected ligands. These computational predictions can help prioritize candidate compounds for further investigation; however, they should not be considered definitive evidence of safety or biological efficacy and must be validated through experimental studies.

Molecular dynamics simulation of the MexB protein

MD simulations were performed for 25 ns to evaluate the structural stability of the MexB protein. The RMSD profile showed an initial increase during the early stage of the simulation, followed by fluctuations within approximately 0.4-0.5 nm for the remainder of the simulation. This pattern indicates that the protein underwent conformational adjustments before reaching a relatively stable dynamic state (Figure 5A).

The RMSF analysis demonstrated generally low residue fluctuations across most of the protein, with pronounced peaks observed only in a limited number of residues corresponding to flexible loop regions (Figure 5B). These localized fluctuations are consistent with the intrinsic flexibility commonly observed in protein structures. The Rg remained relatively stable throughout the simulation, fluctuating between 3.70 and 3.80 nm, suggesting that the overall compactness of the protein was maintained during the simulation period (Figure 5C).

The number of intramolecular hydrogen bonds exhibited moderate fluctuations but remained within a relatively narrow range throughout the simulation, indicating the preservation of the internal hydrogen-bonding network and the structural integrity of the protein (Figure 5D). The SASA initially decreased, followed by minor fluctuations, and eventually stabilized toward the end of the simulation. This behavior suggests only limited changes in solvent exposure during the simulation period (Figure 5E).

Overall, the MD simulation indicated that the modeled MexB protein maintained its structural integrity throughout the 25 ns simulation period. These findings support the protein's structural stability under the simulated conditions. However, these results should be interpreted with caution due to the limited simulation duration. Longer simulations, combined with protein-ligand complex MD analyses, are required to further evaluate ligand-induced stability.

DISCUSSION

The present study demonstrated a high prevalence of MDR *P. aeruginosa* among the investigated clinical isolates, confirming the increasing therapeutic challenges posed by this opportunistic pathogen. The observed resistance patterns align with previous reports describing the widespread dissemination of MDR *P. aeruginosa* in hospital settings, largely attributed to the combined effects of intrinsic resistance mechanisms, target modifications, and multidrug efflux systems. These findings further emphasize the urgent need to identify alternative antibacterial targets and develop novel therapeutic strategies against MDR isolates.[23]

In the present study, molecular detection confirmed the presence of the *GyrB* and *MexB* genes among the investigated isolates, supporting their importance as conserved resistance-associated targets. Furthermore, phylogenetic analysis demonstrated that the representative GyrB sequences clustered with reference *P. aeruginosa* strains, confirming the high conservation of this target and supporting its suitability for target-based computational drug discovery. Similar findings have been reported in previous studies investigating resistance determinants in *P. aeruginosa*, where GyrB and MexB were identified as critical proteins involved in bacterial survival and antimicrobial resistance.[23,24]

Protein modeling and validation demonstrated high structural quality of the generated GyrB and MexB models, as evidenced by MolProbity analysis, Ramachandran plot assessment, and SWISS-MODEL quality metrics. Reliable structural models are essential for obtaining meaningful molecular docking predictions, and similar computational approaches have been successfully employed in previous studies targeting bacterial resistance proteins.[14,25,26]

Molecular docking analysis revealed that the reference inhibitor novobiocin exhibited the strongest predicted binding affinity toward GyrB (-10.2 kcal/mol), consistent with its well-established inhibitory activity against bacterial DNA gyrase. The coumarin derivative also demonstrated favorable predicted binding within the same ATP-binding pocket (-8.2 kcal/mol). Protein-ligand interaction analysis showed that both compounds shared key interactions with Phe460 and Arg391, suggesting a comparable predicted binding mode. However, the coumarin derivative exhibited fewer predicted interactions and a lower predicted binding affinity than the reference inhibitor. These observations align with previous reports describing the gyrase inhibitory potential of coumarin derivatives.[27-29]

Similarly, docking analysis of MexB showed that the reference inhibitor PAbN exhibited the strongest predicted binding affinity within the substrate-binding cavity (-8.1 kcal/mol). The indole derivative displayed a comparable predicted binding orientation, with a docking score of -7.7 kcal/mol, and interacted with several key residues, including Ser352, Asn351,

and Arg358. These findings align with previous studies identifying indole derivatives as promising scaffolds for developing antibacterial agents and efflux pump inhibitors.[30] Nevertheless, it is important to note that molecular docking results are computational predictions of binding behavior and should not be interpreted as direct evidence of inhibitory activity.

The in silico ADMET analysis indicated that both candidate ligands satisfied Lipinski's rule of five without any violations and exhibited favorable predicted physicochemical properties, including high GI absorption and acceptable bioavailability scores. The indole derivative was predicted to be negative for AMES mutagenicity, hepatotoxicity, hERG I/II inhibition, and skin sensitization, whereas the coumarin derivative showed a positive AMES prediction despite its otherwise favorable pharmacokinetic profile. Therefore, the predicted mutagenic liability of the coumarin derivative should be carefully considered and requires further experimental validation. Overall, these in silico ADMET results provide a preliminary computational assessment for prioritizing candidate compounds and should not be interpreted as direct evidence of safety or biological efficacy.[18,31,32]

Based on docking and in silico ADMET analyses, MD simulations were performed to evaluate the structural stability of the modeled MexB protein under simulated physiological conditions. The RMSD profile demonstrated an initial structural adjustment followed by stabilization during the 25 ns simulation period, indicating acceptable complex stability. RMSF analysis revealed limited residue fluctuations except within flexible loop regions, whereas the Rg remained relatively constant, suggesting preservation of protein compactness. The intramolecular hydrogen-bonding network and SASA profile also remained stable throughout the simulation. Collectively, these findings support the structural stability of the modeled MexB protein under the simulated conditions. However, these computational findings should be regarded as preliminary and require further validation through longer MD simulations and experimental antibacterial and efflux pump inhibition studies before definitive conclusions regarding biological activity can be drawn.[33,34]

CONCLUSION

The present study combined clinical microbiology with molecular modeling and in silico approaches to investigate candidate compounds targeting MDR *P. aeruginosa.* The high prevalence of antimicrobial resistance among clinical isolates highlights the urgent need for alternative therapeutic strategies. Molecular analysis confirmed the presence of the *GyrB* and *MexB* genes, while phylogenetic analysis demonstrated the conservation of the GyrB gene among the investigated isolates, supporting its suitability as a target for computational drug discovery.

Molecular docking and in silico analyses indicated that the coumarin and indole derivatives exhibited favorable predicted binding affinities to the GyrB and MexB proteins, respectively. The in silico ADMET evaluation suggested acceptable predicted pharmacokinetic properties for both compounds; however, the coumarin derivative showed a positive AMES test prediction, warranting further investigation. MD simulations confirmed the structural stability of the modeled MexB protein under the simulated conditions.

Overall, these findings provide preliminary molecular modeling evidence supporting further investigation of coumarin and indole derivatives as candidate compounds targeting GyrB and MexB in MDR *P. aeruginosa*. However, these in silico predictions should be considered hypothesis-generating and require experimental validation through in vitro and in vivo studies before definitive conclusions regarding antibacterial or efflux pump inhibitory activity can be drawn.

Highlights

- GyrB and MexB have been identified as conserved therapeutic targets in multidrug-resistant *P. aeruginosa.*
- Novobiocin and PAβN showed the strongest predicted docking affinities against GyrB and MexB, respectively.
- The coumarin derivative demonstrated favorable predicted binding affinity within the GyrB ATP-binding pocket.
- The indole derivative demonstrated favorable predicted binding to the MexB protein.
- In silico ADMET analysis suggested favorable

predicted pharmacokinetic properties for the indole derivative.

- Molecular dynamics simulations supported the structural stability of the modeled MexB protein.

ACKNOWLEDGMENTS

The author gratefully acknowledge the College of Medicine, University of Kufa, particularly the Postgraduate Molecular Biology Laboratory, Department of Microbiology, for providing the laboratory facilities and research environment necessary to conduct this research. The author also expresses gratitude to the University of Arkansas for Medical Sciences (UAMS), USA, for providing access to the WebGRO platform, which was utilized to perform GROMACS-based molecular dynamics simulations in this study.

FUNDING

None.

DATA AVAILABILITY

The nucleotide sequence of the *GyrB* gene was deposited in the DNA Data Bank of Japan (DDBJ) under accession number LC919849, and the corresponding protein sequence has been assigned the GenBank accession number BHR60112.1. All other datasets generated or analyzed during this study are included in the manuscript.

ETHICS STATEMENT

This study was approved by the Medical Ethics Committee, Faculty of Medicine, University of Kufa, Iraq (Approval No. MEC-169, dated 19 May 2025).

REFERENCES

1. Avakh A, Grant GD, Cheesman MJ, Kalkundri T, Hall S. The Art of War with *Pseudomonas aeruginosa*: Targeting Mex Efflux Pumps Directly to Strategically Enhance Antipseudomonal Drug Efficacy. *Antibiotics*. 2023;12(8):1304. doi: 10.3390/antibiotics12081304
2. Abdallah EM, Alhudhaibi AM, Dahab M, et al. The WHO priority list of antibiotic-resistant bacteria: Challenges and opportunities for next-generation antimicrobial development. *Front Pharmacol.* 2026;17:1699987. doi: 10.3389/fphar.2026.1699987
3. Nanjan P, Bose BV. *In silico* Screening of Plant Compounds to Inhibit MexB Efflux Protein for the Enhancement of Meropenem Resistance against *Pseudomonas aeruginosa* MDR Infections. *Recent Adv Antiinfect Drug Discov*. 2025;20(3):223-250. doi: 10.2174/0127724344337172504041142364. Al-Masoodi AKF, Jasim IA. Molecular Identification of MexB Efflux Pump Gene in Clinical Isolates of Pseudomonas aeruginosa. *J Pioneer Med Sci.* 2025;14(5):110-115. doi: 10.47310/jpms2025140517
5. Perera L, Garcia-Villada L, Kaminski AM, Degtyareva N, Pedersen LC, Doetsch PW. Structural and Computational Analysis of Pseudomonas aeruginosa DNA Gyrase Reveals Molecular Characteristics That May Contribute to Ciprofloxacin Resistance. *Biomolecules*. 2026;16(2):318. doi: 10.3390/biom16020318
6. Marinho AM, De Oliveira CM, Silva-Silva JV, et al. Antimicrobial Activity and Molecular Docking Studies of the Biotransformation of Diterpene Acanthoic Acid Using the *Fungus Xylaria* sp. *Antibiotics*. 2023;12(8):1331. doi: 10.3390/antibiotics12081331
7. Gervasoni S, Malloci G, Bosin A, Vargiu AV, Zgurskaya HI, Ruggerone P. Recognition of quinolone antibiotics by the multidrug efflux transporter MexB of *Pseudomonas aeruginosa*. *Phys Chem Chem Phys.* 2022;24:16566–16575. doi: 10.1039/d2cp00951j
8. Alabdali YAJ, Azeez DA, Munahi MG. et al. Molecular Analysis of *Pseudomonas aeruginosa* Isolates with Mutant gyrA Gene and Development of a New Ciprofloxacin Derivative for Antimicrobial Therapy. *Mol Biotechnol*. 2025;67:649-660. doi: 10.1007/s12033-024-01076-y
9. Phan TV, Nguyen VT, Le MT, Nguyen BGD, Vu TT, Thai KM. Identification of efflux pump inhibitors for *Pseudomonas aeruginosa* MexAB-OprM via ligand-based pharmacophores, 2D-QSAR, molecular docking, and molecular dynamics approaches. *Mol Divers*. 2024;28(5):3295-3311. doi: 10.1007/s11030-023-10758-9
10. Dey D, Kavanaugh LG, Conn GL. Antibiotic Substrate Selectivity of *Pseudomonas aeruginosa* MexY and MexB Efflux Systems Is Determined by a Goldilocks Affinity. *Antimicrob Agents Chemother.* 2020;64(8). doi: 10.1128/aac.00496-20
11. Babalola BA, Malik M, Olowokere O, Adebesin A, Sharma L. Indoles in drug design and medicinal chemistry. *Eur J Med Chem Rep.* 2025;13:100252. doi: 10.1016/j.ejmcr.2025.100252
12. Clinical and Laboratory Standards Institute. *Performance standards for antimicrobial susceptibility testing* (35th ed, CLSI Supplement M100). Clinical and Laboratory Standards Institute. 2025.
13. Al-Draghi WA. Molecular Detection of MexA, MexB Efflux Pump Genes and MexR Regulatory Gene in Clinical Isolates of *Pseudomonas aeruginosa*. *Iraqi J Biotechnol.* 2024;23(2)
14. Waterhouse A, Bertoni M, Bienert S, et al. SWISS-MODEL: homology modelling of protein structures and complexes. *Nucleic Acids Res*. 2018;46(W1):W296–W303. doi: 10.1093/nar/gky427
15. Kim S, Chen J, Cheng T, et al. PubChem 2023 update. *Nucleic Acids Res*. 2023;51(D1):D1373-D1380. doi: 10.1093/nar/gkac956

16. Liu Y, Yang X, Gan J, Chen S, Xiao ZX, Cao YX. CB-Dock2: improved protein-ligand blind docking by integrating cavity detection, docking and homologous template fitting. *Nucleic Acids Res*. 2023;50(W1):W159–W164. doi: 10.1093/nar/gkac394
17. Yang X, Liu Y, Gan J, Xiao ZX, Cao Y. FitDock: protein-ligand docking by template fitting. *Brief Bioinform*. 2022;23(3):bbac087. doi: 10.1093/bib/bbac087
18. Daina A, Michielin O, Zoete V. SwissADME: A free web tool to evaluate pharmacokinetics, drug-likeness and medicinal chemistry friendliness of small molecules. *Sci Rep.* 2017;7(1):42717. doi: 10.1038/srep42717
19. Pires DE, Blundell TL, Ascher DB. pkCSM: Predicting Small-Molecule Pharmacokinetic and Toxicity Properties Using Graph-Based Signatures. *J Med Chem*. 2015;58(9):4066-4072. doi: 10.1021/acs.jmedchem.5b00104
20. Abraham MJ, Murtola T, Schulz R, et al. GROMACS: High performance molecular simulations through multi-level parallelism from laptops to supercomputers. *SoftwareX*. 20231-2:19-25. doi: 10.1016/j.softx.2015.06.001
21. IBM Corp. IBM SPSS Statistics for Windows (29). versions 29, 29.0.1. 2022. https://www.ibm.com/docs/en/spss-statistics/29.0.0?topic=overview-whats-new-in-versions-29-2901
22. McHugh ML. The Chi-square test of independence. *Biochemia Medica*. 2013;23(2):143. doi: 10.11613/BM.2013.018
23. Hu M, Chua SL. Antibiotic-Resistant *Pseudomonas aeruginosa*: Current Challenges and Emerging Alternative Therapies. *Microorganisms*. 2025;13(4):913. doi: 10.3390/microorganisms13040913
24. Yin C, Alam MZ, Fallon JT, Huang W. Advances in Development of Novel Therapeutic Strategies against Multi-Drug Resistant *Pseudomonas aeruginosa. Antibiotics*. 2024;13(2):119. doi: 10.3390/antibiotics13020119
25. Bertoni M, Kiefer F, Biasini M, Bordoli L, Schwede T. Modeling protein quaternary structure of homo- and hetero-oligomers beyond binary interactions by homology. *Sci Rep.* 2017;7(1):10480. doi: 10.1038/s41598-017-09654-8
26. Williams CJ, Headd JJ, Moriarty NW, et al. MolProbity: More and better reference data for improved all-atom structure validation. *Protein Science*. 2018;27(1):293-315. doi: 10.1002/pro.3330
27. Al-Khafaji AM, Al-Fatlawy H. Molecular Genotyping of *gyrA,* bla_{OXA-51}, and bla_{OXA-23} Genes in Multidrug-Resistant *Acinetobacter baumannii* Isolated from Childhood Asthma Patients in Iraq. *Egypt J Med Microbiol.* 2025;34(4):483-489. doi: 10.21608/ejmm.2025.386369.1658.
28. Peter S, Sibali LL. Recent Developments on Coumarin Hybrids as Antimicrobial Agents. *Antibiotics*. 2025;14(12):1226. doi: 10.3390/antibiotics14121226
29. Chauhan SS, Thaseen EA, Parthasarathi R. Computational discovery of potent *Escherichia coli* DNA gyrase inhibitor: Selective and safer novobiocin analogues. *Comput Toxicol*. 2024;29:100302. doi: 10.1016/j.comtox.2024.100302
30. Hassan EA, Shehadi IA, Elmaghraby AM, Mostafa HM, Zayed SE, Abdelmonsef AH. Synthesis, Molecular Docking Analysis and in Vitro Biological Evaluation of Some New Heterocyclic Scaffolds-Based Indole Moiety as Possible Antimicrobial Agents. *Front Mol Biosci*. 2022;8:775013. doi: 10.3389/fmolb.2021.775013
31. Bakchi B, Krishna AD, Sreecharan E, et al. An overview on applications of SwissADME web tool in the design and development of anticancer, antitubercular and antimicrobial agents: A medicinal chemist's perspective. *J Mol Struct.* 2022;1259:132712. doi: 10.1016/j.molstruc.2022.132712
32. Karoui S, Khaoua O, Benbellat N, Antonczak S, Messaoudi A. Molecular Docking, Molecular Dynamics, pkCSM Drug Likeness Profiles, Toxicity, and DFT Study of the Antioxidant and Anticancer Activities of Three Flavonoid Derivatives. *ChemistrySelect.* 2024;9(40). doi: 10.1002/slct.202401776
33. Iesce F, Nelen J, Rodriguez-Martinez, A, et al. Discovery of Novel Molecular Scaffolds to Overcome *Pseudomonas aeruginosa* Aminoglycoside Resistance: Insights for a Consensus Scoring Rational Design Approach. *Int J Mol Sci.* 2025;27(6):2642. doi: 10.3390/ijms27062642
34. Krishnamoorthy AS, Bhavya SG, Chandrasekaran R, Palani S, Kuppusamy G, Aasaithambi K. Computational analysis of LasR inhibitors: A novel approach to disrupt quorum sensing in *Pseudomonas aeruginosa*. *In Silico Research in Biomedicine*. 2025;2:100328. doi: 10.1016/j.insi.2026.100328